Plant Physiology and Biochemistry 135 (2019) 359–371

Contents lists available at ScienceDirect

Plant Physiology and Biochemistry

journal homepage: www.elsevier.com/locate/plaphy

Research article

Hydrogen sulfide directs metabolic flux towards the lignan biosynthesis in *Linum album* hairy roots

Safieh Fakhari[a], Mohsen Sharifi[a,*], Roberto De Michele[b], Faezeh Ghanati[a], Naser Safaie[c], Ehsan Sadeghnezhad[a]

[a] Department of Plant Biology, Faculty of Biological Sciences, Tarbiat Modares University, Tehran, Iran
[b] Institute of Biosciences and Bioresources, Italian National Research Council, Palermo, 90129, Italy
[c] Department of Plant Pathology, Faculty of Agriculture, Tarbiat Modares University, Tehran, Iran

ARTICLE INFO

Keywords:
Hairy root
Hydrogen sulfide
Linum album
Phenylpropanoid
Signaling

ABSTRACT

Hydrogen sulfide (H_2S) has been recently found as an important signaling molecule especially in root system architecture of plants. The regulation of root formation through H_2S has been reported in previous works; while the profiling of metabolites in response to H_2S is not clearly discussed. To this end, different concentrations of sodium hydrosulfide (an H_2S donor) were applied to the culture of *Linum album* hairy roots. Subsequently, the amino acid profiles, soluble carbohydrates, and central intermediates of phenylpropanoid pathway with two branches of lignans and flavonoids were assessed by spectroscopy and high performance liquid chromatography techniques. An analysis of the signaling molecules (nitric oxide, hydrogen peroxide, and salicylic acid) was also conducted as they proposed to act in conjunction with H_2S. The H_2S activated antioxidant systems and caused a shift from flavonoid to lignan production (podophyllotoxin and 6-methoxypodophyllotoxin); although, some of the flavonoids increased in a dose-dependent manner. The H_2S decreased the contents of phenylalanine and tyrosine as substrates of the phenylpropanoid pathway, but increased proline and histidine as an osmolyte and antioxidant, respectively. These findings propose that H_2S modulates other signaling molecules, regulates free amino acids, and mediates biosynthesis of lignans and flavonoids in the phenylpropanoids biosynthesis pathway.

1. Introduction

Hydrogen sulfide (H_2S) is a small and water-soluble molecule that freely diffuses through cell membranes. Plants can actively synthesize it under biotic or abiotic stress conditions (Yamasaki and Cohen, 2016). H_2S is involved in many biological processes such as seed germination under stress conditions (Zhang et al., 2008), heat stress tolerance (Li et al., 2013), root organogenesis (Zhang et al., 2009), and cellular adaptive responses to boron (Wang et al., 2010). Similar to the well-characterized nitric oxide (NO), the H_2S acts as a double-edged sword in cell growth and development. The low H_2S concentrations play a protective role in plants under environmental stresses, while at high concentrations it leads to H_2S toxicity through inhibiting the mitochondrial electron transport chain (Dorman et al., 2002; Li, 2013; Zhang et al., 2017). In general, the stimulators affect the cells in a dose dependent manner such that they cause the cell death at the upper limit and play the signaling role at the lower limit. At the moderate level, they induce the biosynthesis of secondary metabolites in order to improve the cell tolerance to biotic and abiotic stresses (Namdeo, 2007).

The H_2S toxicity can inhibit primary root growth by triggering a signal transduction pathway involved with reactive oxygen species (ROS) and NO production (Zhang et al., 2017). However, the mechanisms underlying H_2S signaling on the inhibition of root growth are still unclear. De Michele et al. (2009) demonstrated that NO acts upstream of H_2O_2 in cadmium-induced programmed cell death. In response to stress, ROS lead to oxidative stress, damage of cellular membranes, proteins, carbohydrates, and DNA (Das and Roychoudhury, 2014).

The induction of antioxidant systems, such as the up-regulation of the superoxide dismutase (SOD), catalase (CAT), and guaiacol peroxidase (GPX), is considered as one of the general response mechanisms to stress (Apel and Hirt, 2004). Non-enzymatic antioxidant molecules, such as phenolic compounds, also scavenge ROS and avoid oxidative damage (Zheng and Wang, 2001). The ROS and NO are involved in

Abbreviations: Fresh weight, FW; Hydrogen peroxide, H_2O_2; Hydrogen sulfide, H_2S; Nitric oxide, NO; Phenylalanine ammonia-lyase, PAL; Podophyllotoxin, PTOX; 6-Methoxy podophyllotoxin, 6-MPTOX; Salicylic acid, SA; Sodium hydrosulfide, NaHS; Tyrosine ammonia-lyase, TAL

* Corresponding author.
E-mail address: msharifi@modares.ac.ir (M. Sharifi).

https://doi.org/10.1016/j.plaphy.2018.12.015
Received 24 September 2018; Received in revised form 16 December 2018; Accepted 17 December 2018
Available online 18 December 2018
0981-9428/

elicitor-induced primary and secondary metabolite biosynthesis (Zafari et al., 2016, 2017). The NO is a known elicitor of secondary metabolites such as tanshinone (Du et al., 2015), baicalin (Zhang et al., 2014), taxanes (Wang et al., 2006) and artemisinin (Zheng et al., 2008) in plant tissue cultures. Based on the similarity between the signalling pathways of NO and H_2S (Hu et al., 2014) and the fact that H_2S is able to induce the generation of ROS and NO, it was presumed that H_2S can be involved with the metabolite accumulation by activation of other signaling cascades in plant roots.

Linum album is a medicinal plant with the capability to accumulate some metabolites such as podophyllotoxin (PTOX) and 6-methoxy podophyllotoxin (6-MPTOX) (Esmaeilzadeh Bahabadi et al., 2014; Federolf et al., 2007). These compounds are precursors of such semi-synthetic drugs as etoposide, etopophos, and teniposide with antiviral and anticancer activities (Gordaliza et al., 2004; Ayres and Loike, 1990). The PTOX and 6-MPTOX belong to lignans and are synthesized by the phenylpropanoid pathway to serve as chemical and physical barriers for plant defense responses. It is known that the lignan biosynthetic pathway is linked to phenolic acids derived from hydroxycinnamic acids such as *p*-coumaric, ferulic, and sinapic acids (Peterson et al., 2010). Flavonoids, as the other main branch of the phenylpropanoid pathway, play a variety of biological activities in plants including the defense against pathogens, herbivores, and environmental stresses (Falcone Ferreyra et al., 2012; Shimoi et al., 1996; Soobrattee et al., 2005). In addition, amino acids and carbohydrates can act as signaling molecules in plant defense responses and support energy production based on changes in the interplay between microbes and their hosts (Kadotani et al., 2016; Bolton, 2009). In the present work, the functional role of H_2S in *L. album* hairy root cultures was investigated to understand the H_2S signaling. To this end, the profiles of primary and secondary metabolites were measured in response to the different concentrations of sodium hydrosulfide (as an H_2S donor), with the main focus on the flavonoids and lignans' biosynthetic pathway.

2. Materials and methods

2.1. Hairy roots culture of L. album

The hairy roots of *L. album* were cultured as described previously (Ahmadian Chashmi et al., 2013). At first, the liquid MS culture medium (Murashige and Skoog, 1962) was adjusted to pH 5.8 and then sterilized at 121 °C for 20 min. The stock cultures were grown in 250 mL Erlenmeyer flasks with a working volume of 50 mL. The hairy roots were grown in 250 mL Erlenmeyer flasks on orbital shaker incubator (100 rpm, 25 °C) in darkness. The suspension culture was sub-cultured every 3 weeks in flasks containing 50 mL of the liquid MS medium supplemented with 3% sucrose under similar operating conditions.

2.2. NaHS treatment in hairy roots culture of L. album

The hairy roots (2 g FW) were transferred to a 100 mL Erlenmeyer flask containing 30 mL MS culture medium supplemented with 3% sucrose. The H_2S donor, NaHS, was added to the media after 11 days following sub-culturing at three different concentrations (0.5, 1, and 2 mM). The NaHS was dissolved in deionized water and filter-sterilized before adding to the culture medium. The incubation of these cultures continued on an orbital platform shaker for 5 days after NaHS treatment. The cultures were then harvested by filtration, weighted, and immediately frozen in liquid nitrogen for further analysis.

2.3. Determination of H_2S content

Hydrogen sulfide in hairy root tissues was determined according to the method described by Xie et al. (2014) with slight modifications. This method is based on the formation of methylene blue from dimethyl-p-phenylenediamine in HCl. In brief, the tissue samples (0.7 g FW) were homogenized in 2.5 mL of Tris-HCl 20 mM) pH 6.8) containing 10 mM ethylene diamine tetra acetic acid (EDTA) and centrifuged at 12000 g for 15 min at 4 °C.

A 0.75 mL aliquot of the supernatant was mixed with 0.2 mL of 1% (w/v) zinc acetate. Then, 20 mM dimethyl-p-phenylenediamine and 30 mM ferric chloride were prepared by 7.2 M HCl and 1.2 M HCl as solvents, respectively. After 30 min, a 0.1 mL aliquot of both dimethyl-p-phenylenediamine (20 mM) and ferric chloride (30 mM) were added to the supernatant fraction. This reaction was incubated at room temperature for 15 min, and the absorbance was recorded at 670 nm. The content of H_2S was calculated by a calibration curve method using NaHS as standard.

2.4. Determination of NO content

The NO content was quantified by determination of nitrite (NO_2^-) using the Griess reagent. Due to facility constraints, the quantitation of NO using Griess reagent was performed indirectly through colorimetric reduction of nitrite. However, we are aware of our results on NO that suffer from cross-reactivity with other metabolites such as nitrite itself. The samples (0.2 g FW) were crushed and extracted with 1.5 mL of 100 mM phosphate buffer (pH 7.0). The homogenate was centrifuged at 10000 g for 15 min at 4 °C. and the supernatant (200 μL) was added to 1800 μL phosphate buffer (pH 7.0) and 0.2 mL of Griess reagent (1% sulfanilamide and 0.1% N-1-napthylethylenediamine dihydrochloride in 5% phosphoric acid solution) at room temperature for 10 min (Green et al., 1982). The sample absorbance was recorded at 540 nm and the NO concentration was measured by the calibration curve for sodium nitrite.

2.5. H_2O_2 content measurement

For determination of H_2O_2 content, the samples (0.25 g FW) were extracted with 2 mL trichloroacetic acid (TCA; 0.1%, w/v) in ice bath and centrifuged at 12000 g for 15 min. An aliquot of 0.1 mL of the extract was mixed with 0.9 mL of 0.1 M potassium iodide (KI) in 1N HCl solution. After 10 min exposure to darkness, the absorbance of the mixture was recorded at 390 nm. The H_2O_2 content was quantified by a calibration curve method (Nahidian et al., 2018).

2.6. Determination of soluble sugars

The quantification of soluble sugars was performed according to DuBois et al. (1956). The samples (0.1 g FW) were homogenized in the 1.5 mL of 0.1 M phosphate buffer (pH 6.8). The homogenate was centrifuged at 12000 g for 20 min, and then 0.5 mL of supernatant was mixed with 0.5 mL of phenol (5%) and 2.5 mL of concentrated sulfuric acid. After 10 min, the absorbance of the mixture was recorded at 480, 485 and 490 nm for soluble sugars. The contents of soluble sugars were expressed as mg g^{-1} FW by a calibration curve.

2.7. Measurement of total amino acids

The contents of free amino acids determined according to the method described by Lee and Takahashi (1966). The samples (0.1 g FW) were extracted with 1 mL 70% ethanol and washed in distilled water. The extract (1 mL) was mixed with 3 mL of 55% glycerol, 0.5 mL of 0.5 M acetate buffer (pH 5.5), and 0.5 mL of ninhydrin solution. For ninhydrin preparation, 1.25 g of ninhydrin was dissolved in 30 mL of glacial acetic acid and 20 mL of phosphoric acid (6 M) with warming and agitation. This mixture was incubated in a boiling water bath for 20 min. Then, the test tubes were cooled rapidly under cold running water. The sample absorbance was measured at 570 nm. The results were expressed as mg g^{-1} sample. Glycine dissolved in 0.5 M citrate buffer (pH 5.6) was used as the standard.

2.8. Determination of proline concentration

The samples (0.5 g FW) were homogenized in 10 mL sulfosalicylic acid (3%) and centrifuged at 3000 g for 10 min. The supernatant was mixed with ninhydrin solution (section 2.7) and 2 mL of glacial acetic acid, and was boiled for 1 h. Then, the reaction mixture was put in the ice bath and the chromophore was extracted with 4 mL toluene. The quantification of the proline-ninhydrin complex in toluene was performed spectrophotometrically at 520 nm (Bates et al., 1973).

2.9. Determination of total phenol and flavonoid contents

For measurement of total phenol content, the method of Akkol et al. (2008) was used to extract phenolic compounds. At first, the samples (0.05 g DW) were homogenized in 8 mL of methanol (80%) and centrifuged at 3000 g for 10 min. Then, 1 mL of methanolic extract was mixed with 5 mL of Folin-Ciocalteu reagent (previously diluted the stock 1:10 with distilled water) and 4 mL of sodium carbonate solution (7.0%). The mixtures were kept for 2 h at room temperature, and then absorbance was measured at 765 nm. Gallic acid was used as standard and the total phenol values were expressed in terms of mg gallic acid equivalent in g of FW. Total flavonoid content was determined by the aluminum chloride method (Akkol et al., 2008). Briefly, 1 mL of methanolic extract of hairy roots was mixed with 250 µL of aluminum chloride. Next, 250 µL of potassium acetate was added and the samples remained at room temperature for 30 min. The absorbance of the reaction mixture was measured at 415 nm.

2.10. Antioxidant enzymes assay

The samples (0.1 g FW) were homogenized in 1.5 mL of 0.1 M phosphate buffer (pH 8) containing 1.0 mM dithiothreitol (DTT) on ice. The homogenate was centrifuged at 12000 g for 30 min at 4 °C. The supernatant was used as a source for enzyme activity assays. The protein concentration of sample was measured by Bradford assay (Bradford, 1976). The SOD activity was assayed according to Giannopolitis and Ries (1977). The absorbance of samples was recorded at 560 nm based on inhibition in the photochemical reduction of nitroblue tetrazolium (NBT). The CAT activity was determined at 240 nm based on the initial rate of disappearance of H_2O_2 for 1 min (Cakmak and Marschner, 1992). The GPX activity was based on the oxidation of guaiacol by hydrogen peroxide and recorded spectrophotometrically at 470 nm (Chance and Maehly, 1955).

2.11. PAL and TAL activity assay

The activity of PAL and TAL enzymes were measured according to the production of cinnamic and p-coumaric acids, respectively. For assay of TAL activity, 0.1 mL of the enzyme extract was added to 0.1 M phosphate buffer (pH 8.8) containing L-tyrosine (0.1 M) and incubated at 37 °C for 1 h. The reaction was stopped by the addition of 0.05 mL of 6 M HCl. The p-coumaric acid content was extracted with 5 mL of ethyl acetate and then evaporated to remove solvent residues. The solid residue was dissolved in 1 mL of NaOH (0.05 M) and the absorbance was measured at 330 nm. For assay of the PAL activity, L-phenylalanine (0.1 M) was used as a substrate and the absorbance was measured at 290 nm. The enzyme activity was defined as µmol of trans-cinnamic acid and p-coumaric acid in mg protein^{-1} h^{-1} for PAL and TAL activity, respectively (Pareek et al., 2017).

2.12. Extraction and quantitative analysis of lignans with HPLC

Lignan extraction and quantification were performed according the method described by Van Uden et al. (1989). The dried sample (100 mg) was dissolved in 4 mL of methanol (80% v/v) and sonicated for 1 h at 4–6 °C. Dichloromethane (4 mL) and water (4 mL) were then added, resulted in two layers. Next, the dichloromethane phase was collected and evaporated at room temperature. The solid residue was dissolved in 1 mL of pure methanol, filtered (0.22 µm pore sizes) and then injected into the HPLC. The quantification of lignans was performed using an UV–vis detector and an ODS-3 C18 (250 mm × 4.6 mm, 5 µm) column with gradient system. The PTOX and 6-MPTOX were detected at 290 nm by comparison of the retention times with reference substance.

2.13. Determination of amino acid profile

In order to extract the amino acids according to the method described by Di Martino et al. (2003), the sample (200 mg FW) was ground in liquid nitrogen, homogenized in 2 mL of ethanol 80% (v/v), and centrifuged at 10000 g for 15 min at 4 °C. The supernatant was evaporated to dryness at room temperature, and the residue was dissolved in 1 mL of water. For amino acid detection, the method of Biermann et al. (2013) was used with slight modifications. The separation of amino acids were carried out by a column (4.6 × 150 mm, 3.5 µm particle size; Agilent Technologies 1260 infinity, USA) and detected with fluorometric detector (FLD). In a reaction vial insert, 50 µL of the sample was derivatized with OPA (40 µL). After 30 s of reaction time, 20 µL of the solution was injected into the column. The column temperature was kept at 40 °C, and flow rate was 0.5 mL min^{-1} when using two solvents gradient elution. The mobile phase A consisted of 25 mM Na_2HPO_4/NaH_2PO_4 (pH 7.2)/tetrahydrofuran (95:5, v/v), and the mobile phase B was a mixture of 25 mM Na_2HPO_4/NaH_2PO_4 (pH 7.2)/methanol/acetonitrile (50:35:15, v/v/v). The peaks were identified by comparison of the retention times with the reference substances.

2.14. Analysis of phenolic acids and flavonoids with HPLC

The detection of phenolic acids was performed according to the method described by Owen et al. (2003). The sample (0.5 g FW) was homogenized in 3 mL of methanol. The solvent was evaporated to dryness under vacuum at 35 °C. The residue was dissolved in acetonitrile (4 mL) and ultimately extracted three times with hexane (3 mL). The hexane layer was discarded and the acetonitrile solution was dried. The solid residue was dissolved in pure methanol (0.5 mL) and injected into the HPLC column ODS-3 C18 (250 mm × 4.6 mm, 5 µm). Detection was performed at 280 and 340 nm and the identification of compounds was confirmed by comparing their retention times with the reference substances. The flavonoids extraction was performed according to the method described by Keinanen et al. (2001). The sample (0.5 g FW) was extracted with 1.5 mL of 40% methanol containing 0.5% acetic acid. Following 4 h of shaking, the mixture was centrifuged at 13000 g for 12 min, and the supernatant absorbance was measured at 254, 280, 300 and 350 nm. The mobile phase composition during the gradient consisted of 0.5% phosphoric acid in acetonitrile (solvent A) and deionized water (solvent B) (Gudej and Tomczyk, 2004). The identification of flavonoids was confirmed by comparing their retention times with the reference substances.

2.15. Statistical analysis

The principal components analysis (PCA) and cluster analysis were performed by MetaboAnalyst (http://www.metaboanalyst.ca), a web server for metabolomics data processing (Clark and Ma'ayan, 2011). In addition, all data were analyzed using Origin 7.0 software (Edwards, 2002). All the experiments were performed in triplicates and the results were presented as the mean ± SE. The statistical analysis was conducted using student's T-test and Tukey's test ($P < 0.05$, $P < 0.01$).

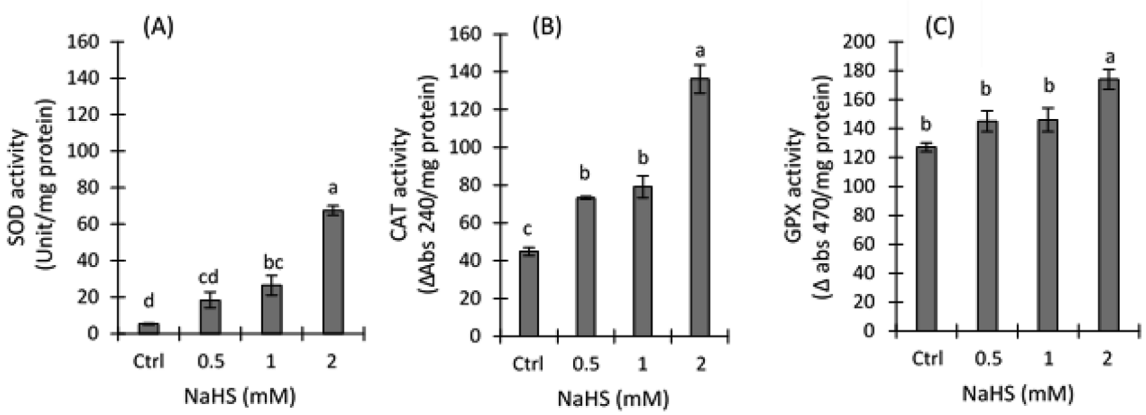

Fig. 1. Changes of SOD (A), CAT (B), and GPX (C) activities with different concentration of NaHS added on day 11 in hairy root culture of *L. album*. All the data are presented as the mean ± SE with n = 3. Means with different letters are significant at P ≤ 0.05 as determined by the Tukey test.

3. Results

3.1. Growth response of hairy roots to NaHS

To determine how exogenous H_2S affects the hairy root growth, 11-day-old hairy roots were treated with 0.5, 1, and 2 mM NaHS. The hairy root growth was measured in dry weight 5 d after exposure (Fig. S1). The hairy root growth was significantly decreased about 7.6%–10.8% in comparison with the controls, when NaHS concentrations increased from 0.5 to 1 mM, respectively. The dry weight of roots with 2 mM NaHS treatment showed no significant changes compared to control.

3.2. Antioxidant defense in NaHS-stressed hairy roots

To understand the effects of H_2S on the oxidative stress response, the activities of three antioxidant enzymes (SOD, CAT and GPX) were determined (Fig. 1A–C). The activities of all three enzymes significantly increased (P ≤ 0.05) at 2 mM NaHS compared to their respective controls. The SOD and CAT activities significantly increased by 4.9- and 1.7-fold at 1 mM NaHS compared to control, respectively, while no significant changes were observed for the GPX activity in this concentration. Furthermore, the CAT activity was significantly enhanced by 1.6-fold at 0.5 mM NaHS treatment when compared to control (Fig. 1B). There was a positive correlation between antioxidant enzymes activities and total phenolic content, but not with lignans and total flavonoids (Table 1). These results showed an increase in the antioxidants such as flavonoids and phenolics at 0.5 and 2 mM NaHS, respectively, whereas no significant changes were observed at 1 mM NaHS (Fig. S2).

3.3. NaHS triggers endogenous H_2S, H_2O_2 and NO production

The effect of exogenous H_2S on the endogenous H_2S concentration in *L. album* hairy roots was tested. In this context, we tested the effect of 1 mM NaHS treatment that had stronger growth-inhibitory effect in hairy roots. As shown in Fig. 2A, the production of endogenous H_2S significantly increased after 4, 8, and 24 h of exogenously applied NaHS compared to control. We trust that the assay detected endogenous H_2S levels rather than residual exogenous treatment with the donor because of the extensive wash of the sample and extraction procedure. In order to understand the crosstalk between H_2S and reactive oxygen and nitrogen species, the production of H_2O_2 and NO was measured after treatment with NaHS. The application of NaHS caused an increase in H_2O_2 levels at 8 h (20%, $p < 0.05$) (Fig. 2B). NO production was an early event since its content significantly increased by 10% and 28% ($p < 0.05$) at 4 and 8 h, respectively, but it returned to control levels after 12 and 24 h post-exposure (Fig. 2C).

3.4. Effects of NaHS treatment on primary metabolites (sugars and amino acids)

Since NaHS significantly affected root growth, we measured primary metabolite contents (amino acids and sugars) to determine the mechanisms of growth impairment in hairy roots. In response to NaHS, the concentrations of glucose and mannose (Figs. S3A and B) did not change significantly. Rhamnose and xylose increased (Fig. S3C) insignificantly by about 8.5% after exposure to 1 mM NaHS compared to control. Total amino acid content increased significantly in the presence of 0.5 and 1 mM NaHS (Fig. S4), while it was similar to control at 2 mM

Table 1
Linear correlations (Pearson's coefficient) among some compounds and enzymes during time after NaHS exposure in *L. album* hairy roots.

Pearson correlation	TAL	PAL	Tyrosine	Phenyl alanine	Caffeic acid	Coumaric acid	Ferulic acid	PTOX	6-MPTOX	Phenol	Flavonoids	CAT	SOD
PAL	−0.168												
Tyrosine	0.263	−0.735**											
Phenylalanine	0.415	−0.795**	0.747**										
Caffeic acid	0.299	0.264	0.240	−0.003									
Coumaric acid	0.923**	−0.122	0.268	0.305	0.340								
Ferulic acid	0.832**	−0.057	0.399	0.266	0.653*	0.868**							
PTOX	−0.105	0.626*	−0.858**	−0.742**	−0.196	−0.036	−0.202						
6-MPTOX	−0.335	0.429	−0.835**	−0.457	−0.624*	−0.358	−0.648*	0.619*					
Phenol	−0.525	−0.609*	0.479	0.352	−0.311	−0.638*	−0.532	−0.516	−0.231				
Flavonoids	−0.027	0.186	−0.673*	−0.110	−0.428	−0.117	−0.374	0.364	0.803**	−0.279			
CAT	−0.670*	−0.329	0.163	0.076	−0.376	−0.807**	−0.741**	−0.298	0.055	0.922**	−0.058		
SOD	−0.702*	−0.386	0.217	0.165	−0.317	−0.808**	−0.703*	−0.347	−0.044	0.925**	−0.108	0.938**	
GPX	−0.780**	−0.239	0.070	0.067	−0.407	−0.820**	−0.780**	−0.373	0.203	0.741**	0.130	0.810**	0.869**

Levels of significance are: **P ≤ 0.01, *P ≤ 0.05.

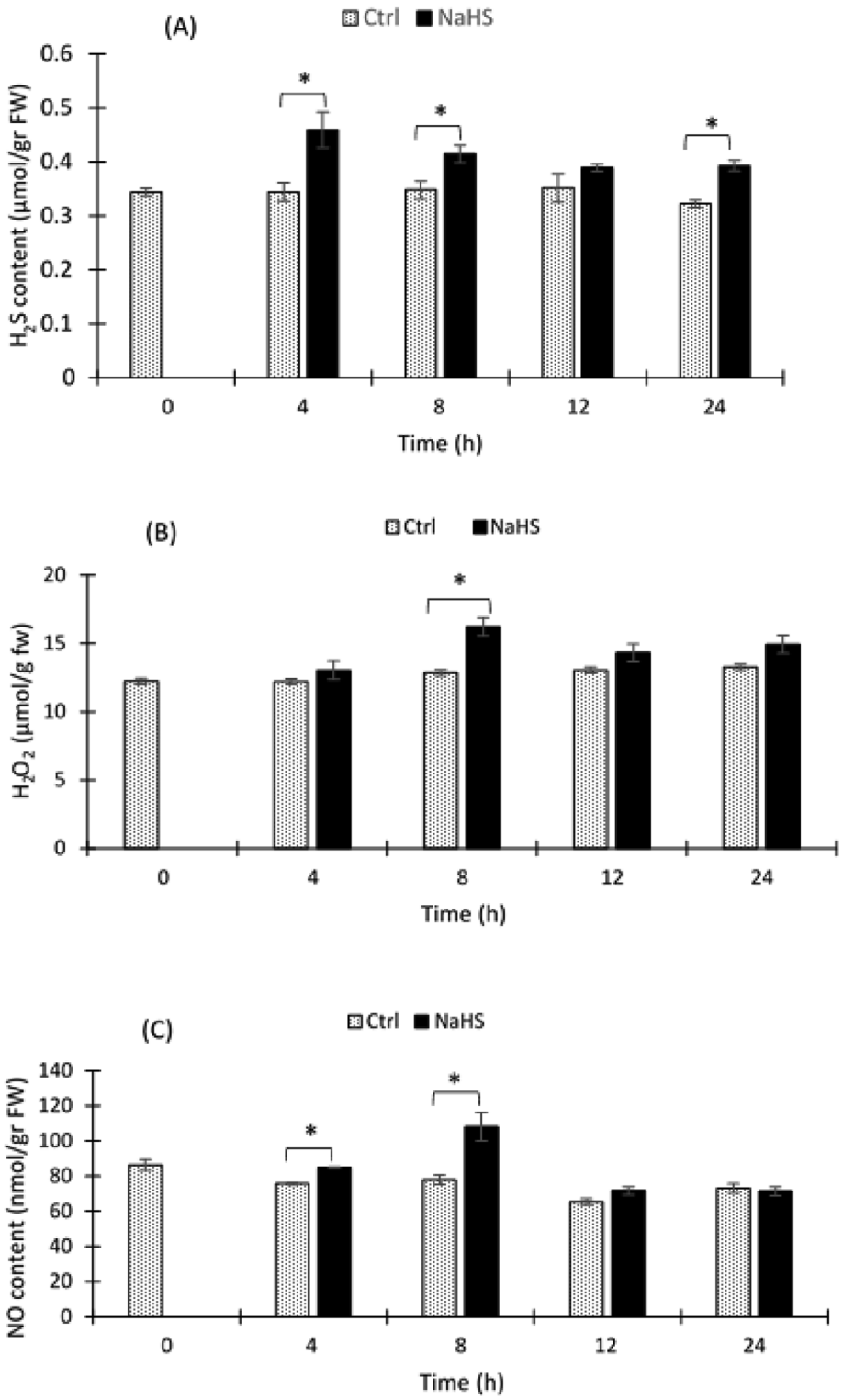

Fig. 2. Effect of the NaHS treatment (1 mM) on H_2S, H_2O_2, and NO levels in hairy roots of *L. album*. All the data are presented as the mean ± SE with n = 3. The significant difference is determined by T-test at $P \leq 0.05$ (*) between control and NaHS-treated cultures.

NaHS. The profiles of seven amino acids (arginine, aspartate, glutamate, serine, phenylalanine, tyrosine, and valine) showed a decrease after addition of NaHS, especially in 1 mM dosage. The contents of proline and histidine were increased significantly at 1 mM NaHS (Fig. 3A, C). In particular, histidine content increased about 8 and 10 fold after treatment with NaHS at concentrations of 1 and 2 mM, respectively.

3.5. H_2S stimulates the phenylpropanoids pathway to portionize the biosynthesis of end products in different branches

In our study, free amino acid profiles showed that the aromatic amino acids, phenylalanine and tyrosine, decreased after addition of 1 mM NaHS (Fig. 3G and H). Since phenylalanine and tyrosine are substrates in the phenylpropanoid pathway, we suspected that phenylpropanoid secondary metabolites are affected by NaHS as well.

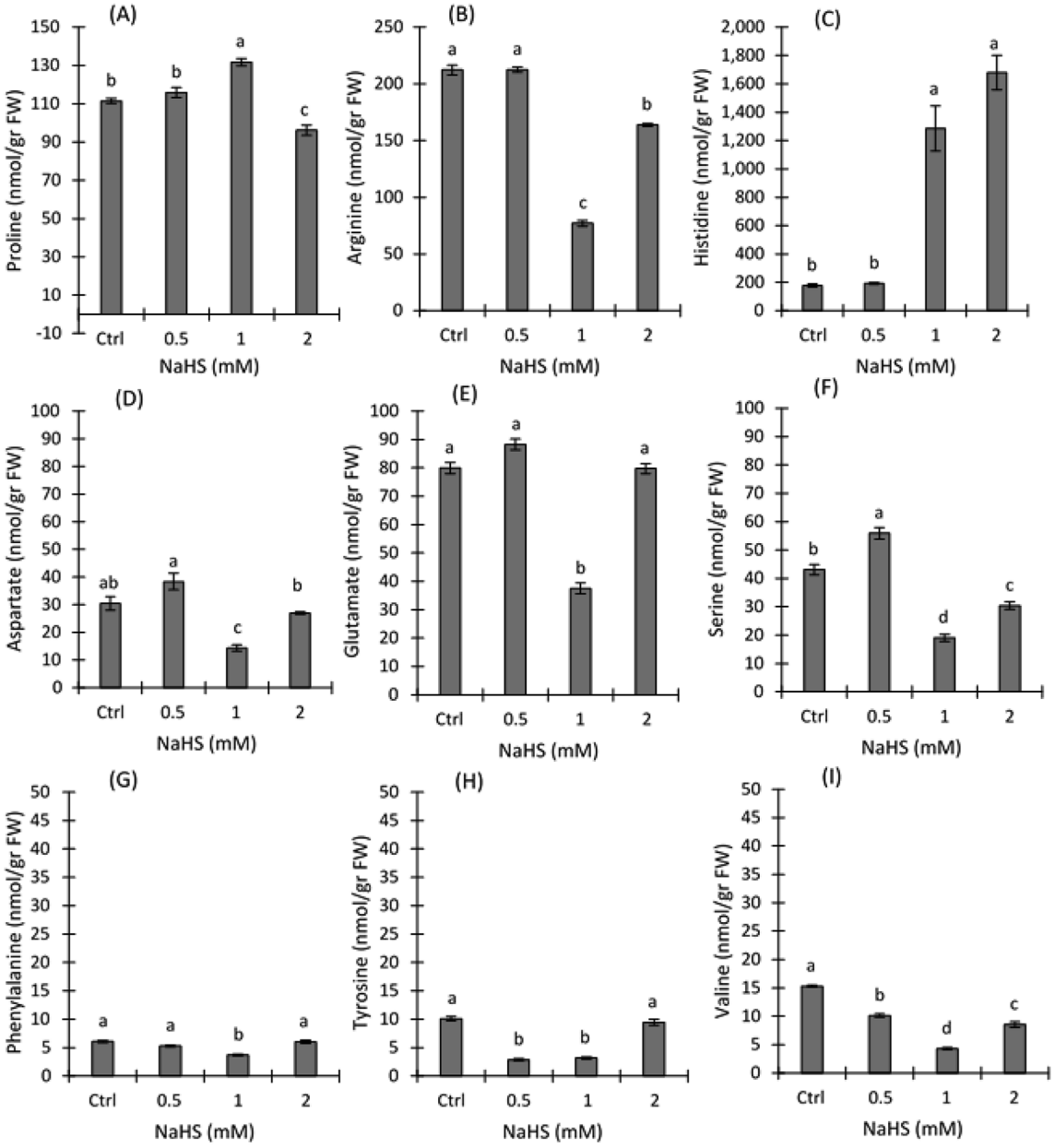

Fig. 3. Changes in the contents of free amino acids in response to the NaHS treatment in hairy roots of *L. album*. All the data are presented as the mean ± SE with n = 3. Means with different letters are significantly different at P ≤ 0.05 as determined by the Tukey test.

Therefore, we measured the activity of key enzymes including PAL and TAL in the pathway. The PAL activity significantly increased in the hairy roots, reaching a maximum (~134% than control) at the concentration of 1 mM NaHS (Fig. 4A). With increasing concentration of NaHS treatment, we observed a significant decrease in the activity of TAL (Fig. 4B).

The NaHS treatment stimulated lignan production in hairy roots of *L. album*. The levels of 6-MPTOX and PTOX reached a maximum under 0.5 and 1 mM NaHS, respectively, but higher concentration of NaHS (2 mM) decreased both of them in hairy root cultures (Fig. 4C and D). As presented in Table 1, there were a statistically significant negative relationship between the PAL activity and tyrosine (r = −0.735), phenylalanine (r = −0.795), and total phenol (r = −0.609), but it had a positive correlation with PTOX (r = 0.626). Moreover, the TAL activity was highly and positively correlated with coumaric acid (r = 0.923) and ferulic acid (r = 0.832).

The HPLC analysis of phenolic acids showed the presence of coumaric acid, caffeic acid, ferulic acid, and SA in the hairy roots of *L. album*. (Fig. 4E). The NaHS treatment decreased the contents of phenolic acids, with the exception of SA. Furthermore, there were significant positive correlations between ferulic acid and both coumaric acid (r = 0.868) and caffeic acid (r = 0.653) (Table 1). The levels of coumaric acid and ferulic acid significantly decreased with increasing concentrations of NaHS from 0.5 to 2 mM. The total content of caffeic acid significantly decreased by both 0.5 mM and 2 mM NaHS, but at 1 mM NaHS was similar to control samples.

Conversely, the SA content increased in the concentration of 1 mM NaHS.

3.6. Flavonoid profiles in hairy roots

Besides lignans, the phenylpropanoid pathway can lead to the synthesis of flavonoids. As presented in Table 1, total flavonoids showed a positive correlation with 6-MPTOX (r = 0.803) and a

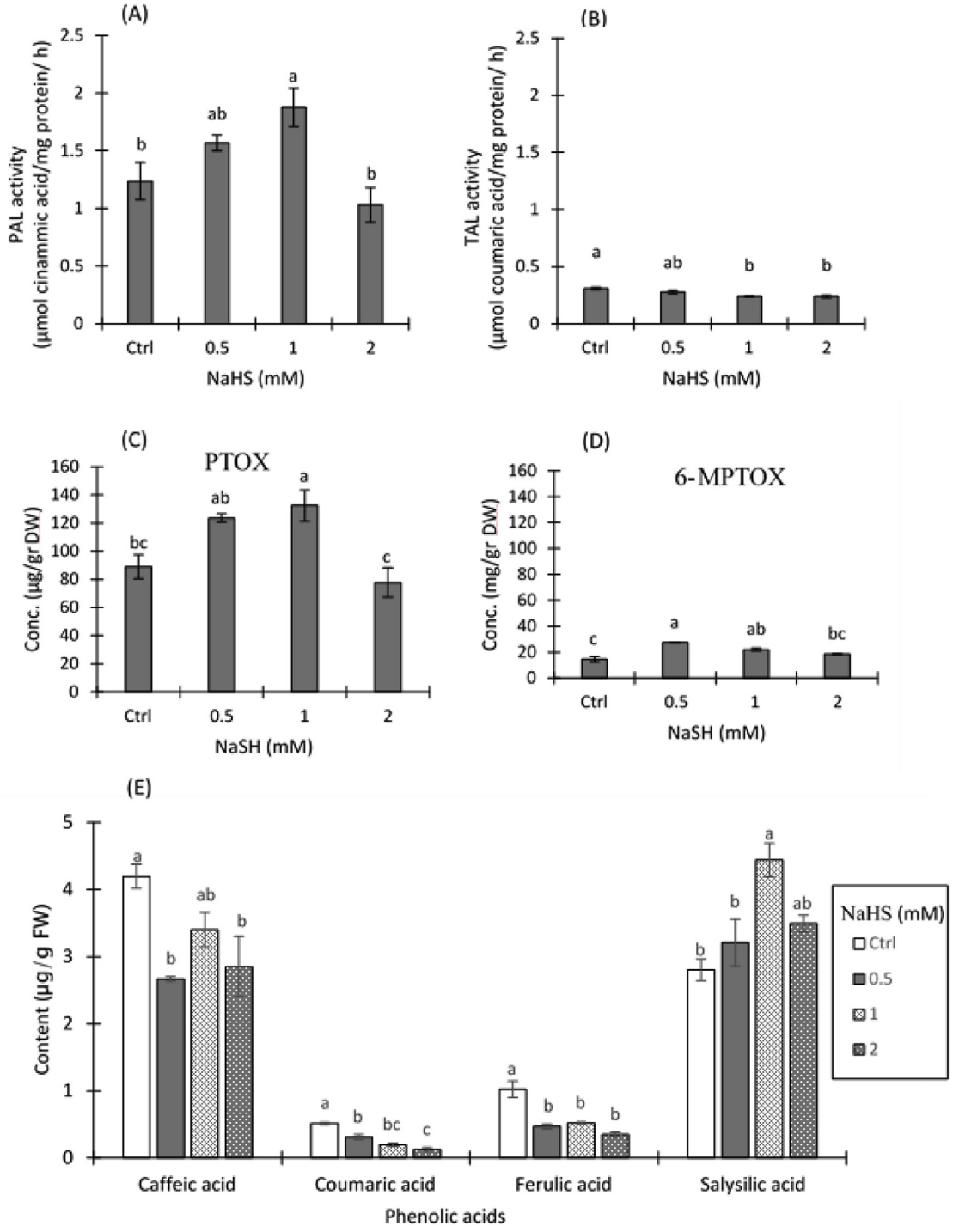

Fig. 4. Effect of the NaHS treatment on the PAL (A) and TAL (B) activities, content of lignans, PTOX (C) and 6-MPTOX (D) and phenolic acids (E). All the data are presented as the mean ± SE with n = 3. Means with different letters are significantly different at $P \leq 0.05$ as determined by the Tukey test.

negative correlation with tyrosine ($r = -0.673$). The PTOX was negatively correlated with both tyrosine ($r = -0.858$) and phenylalanine ($r = -0.742$). There are very few reports about the comprehensive metabolic profile and natural diversity of flavonoids in hairy roots of *L. album*, which we detected by HPLC (Fig. 5). Exposure to 0.5 mM NaHS caused a significant increase in flavonoids contents, including vitexin (17%) and diosmin (61%), and stilbene such as resveratrol (25%) compared to control (Fig. 5C, E, G). Significant decreases were observed in kaempferol (26%), vitexin (20%), daidzein (32%), diosmin (69%), myricetin (35%), resveratrol (21%), and naringenin (37%) at 1 mM NaHS compared to 0.5 mM NaHS (Fig. 5A, C-H), whereas catechin and apigenin did not show significant changes (Fig. 5B, I(after both NaHS treatments. The higher concentrations of NaHS (2 mM) also significantly reduced the flavonoid compositions such as kaempferol (20%), catechin (29%), and naringenin (43%).

3.7. Metabolites classification

When we analyzed the profiles of the primary and secondary metabolites via principal component analysis (PCA), the strong patterns in a subset of the metabolites were observed. The principal components 1 and 2 (PC1 and PC2) accounted for 41.5% and 24% of the total variance

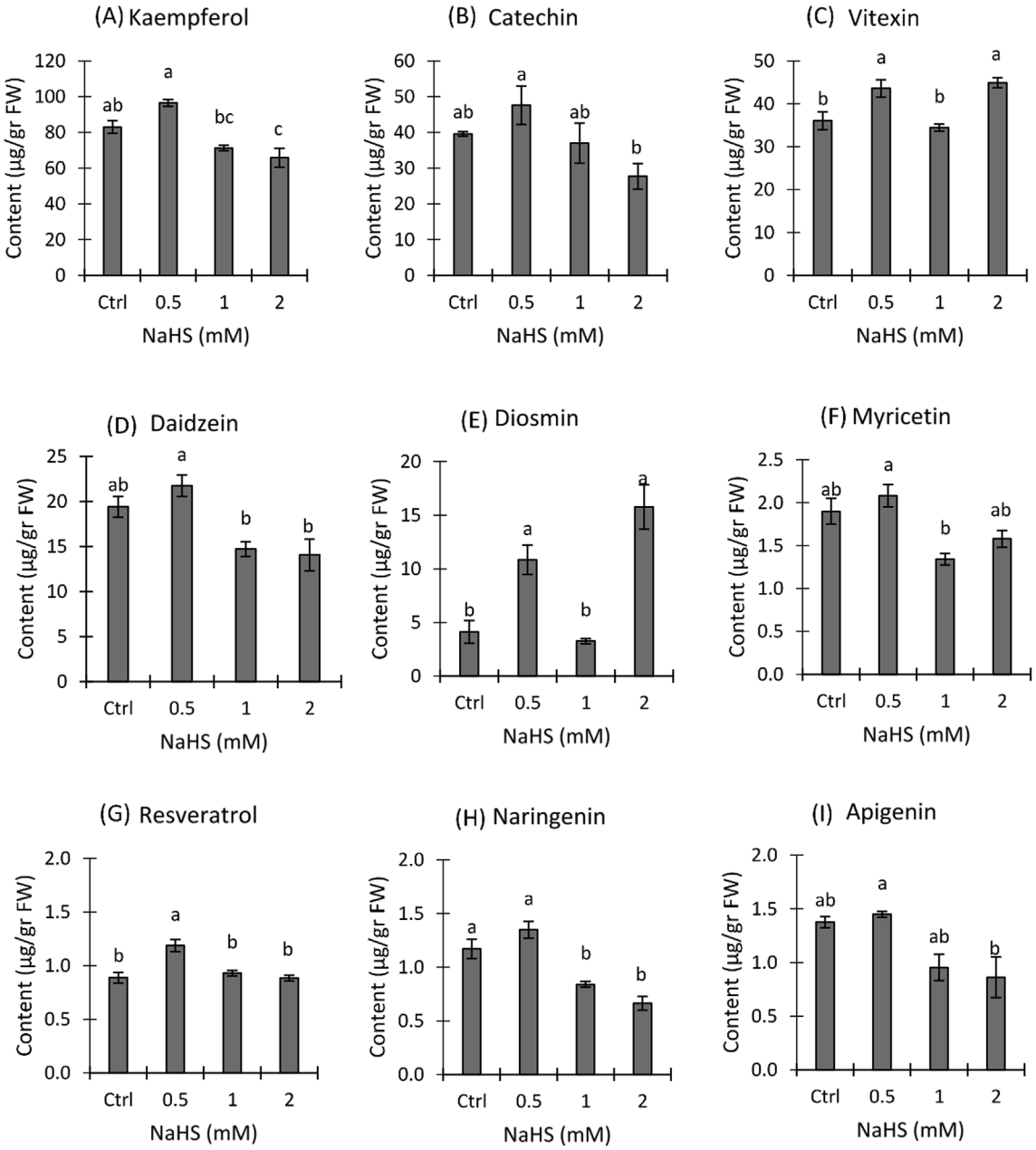

Fig. 5. Identification of flavonoid compositions by HPLC in hairy roots of *L. album*. All the data are presented as the mean ± SE with n = 3. Means with different letters are significantly different at P ≤ 0.05 as determined by the Tukey test.

in the dataset, respectively (Fig. 6A). The two components showed clear segregation according to different concentrations of NaHS including 0.5, 1, and 2 mM after 5 d of exposure.

As shown in Fig. 6B, Pearson's correlation coefficient was calculated between the metabolites in response to NaHS, to classify the compounds according to similar patterns in a clustered heat map. Results showed a strong correlation between the primary and secondary metabolites in samples treated with NaHS and revealed three major clusters (1–3) with different response patterns (indicated on the dendrogram with red color in Fig. 6B) when NaHS concentration was increasing.

The different clusters represent the communication of metabolic pathways through co-grouping of metabolites with each other's; for example, sugars biosynthesis were ultimately coordinated with the lignan biosynthesis such as PTOX and 6-MPTOX, and the end products of the phenylpropanoid pathway, which they were grouped in cluster 1. The phenolic acids (as the central intermediates in the phenylpropanoid biosynthesis) were classified into clusters 2 and 3 including flavonoids and amino acids, respectively. They were derived from aromatic amino acids and converted to flavonoids.

4. Discussion

Exposure of hairy roots of *L. album* to NaHS can activate the biosynthesis of secondary metabolites. The H_2S play the role of a signaling molecule at low concentrations and a toxic substance at high dosage. The H_2S caused a decrease in hairy root growth. In agreement with our findings, Montesinos-Pereira et al. (2016) reported similar decline in the biomass of *Brassica oleracea* after NaHS treatment. The H_2S could also decrease the auxin generation via disrupting the activity of polar auxin transport and inhibition of the primary root growth (Jia et al., 2015). It was also observed that H_2S generation was accompanied by a burst in H_2O_2 and NO. Similarly, Zhang et al. (2017) reported H_2S-dependent ROS accumulation and its inhibitory effect on plant root

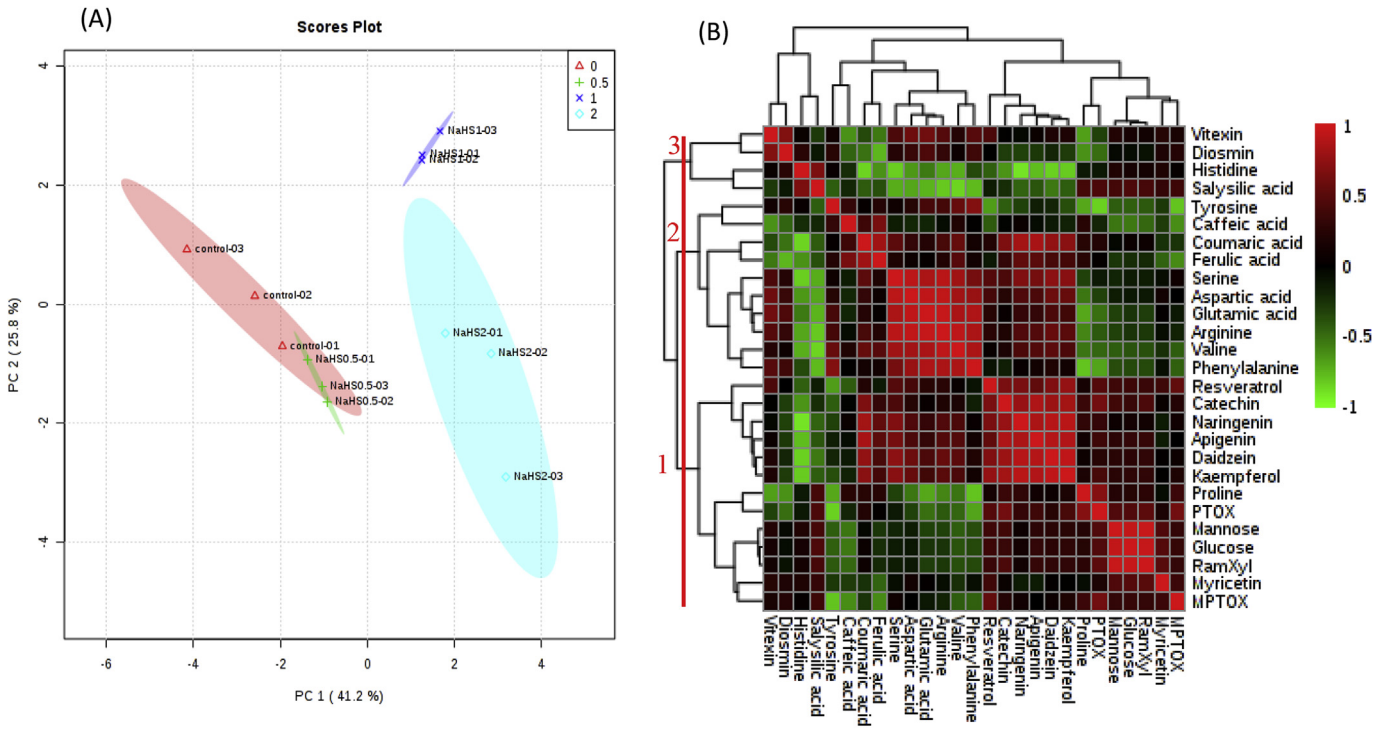

Fig. 6. Metabolites classification in the treatment of hairy roots of *L. album* with NaHS. **(A)** Scores plots of principal component analysis (PCA) using metabolite data belonged to 15-day-old hairy roots. **(B)** Pearson correlation coefficient of each metabolite with others in the heat map graph. Colors in the matrix boxes show the magnitude and direction of the correlations: intense green and red indicate strong negative and positive correlations, respectively. Red line shows the components and number of metabolites classification. (For interpretation of the references to color in this figure legend, the reader is referred to the Web version of this article.)

growth. On the other hand, the H_2S can stimulate the antioxidant machinery and alleviate toxicity symptoms. Wang et al. (2010) found that the NaHS alleviates the inhibitory effect of boron on root elongation in cucumber seedlings. Ge et al. (2017) showed that H_2S delays plant senescence by alleviating oxidative damage. In our study, the NaHS treatment up-regulated and increased the activities of CAT, SOD, and GPX in the hairy roots of *L. album*.

4.1. Interaction between H_2S and other signaling molecules

In different experiments, it was shown that H_2S can act upstream or downstream of other signal molecules including such hormones as indole acetic acid (Zhang et al., 2009), gibberellic acid (Xie et al., 2014), jasmonic acid (Chen et al., 2016), and SA (Li et al., 2015), and such bioactive compounds as NO (Wang et al., 2012; Shi et al., 2014) and ROS (Hancock and Whiteman, 2014). The H_2S stimulates the biosynthesis of SA via activation transcripts of enhanced disease susceptibility$_1$ (EDS_1) and phytoalexin deficient$_4$ (PAD_4), both responsible for the SA generation in Arabidopsis (Shi et al., 2015). In addition, the SA increases cysteine and sulfur contents (Pál et al., 2014; Nazar et al., 2015; Hasanuzzaman et al., 2018), and the SA homeostasis is regulated by a sulfo-transferase (SOT12) via sulfation (Baek et al., 2010). Zottini et al. (2007) showed the dose-dependent induction of NO synthesis by SA in Arabidopsis; therefore the SA can act upstream of NO. The regulatory role of NO on the key regulators of the SA signaling pathway, TGA1 and NPR1, shows that the translocation of NPR1 into the nucleus is promoted by NO and is a prerequisite for the SA-induced redox changes (Lindermayr et al., 2010; Tada et al., 2008).

Different stresses, including salinity and heat stress could create the similar results in barley seedling roots (Chen et al., 2015) and Zea mays (Zg et al., 2013) respectively. Overall, both NO and H_2S can promote plant tolerance to abiotic stress (Hasanuzzaman et al., 2018). The NaHS also triggers the accumulation of H_2O_2 in lateral root development of tomato seedlings (Mei et al., 2017). In the present work, it was also observed that the NaHS causes a peak in the H_2O_2 production 8 h after treatment.

4.2. H_2S regulates the metabolic roles of free amino acids

Amino acids play essential roles as building blocks of proteins, source of energy, and precursors of secondary metabolites. The changes occurring in the contents of the free amino acids in response to the NaHS treatment suggest the involvement of amino acid metabolism in defense responses of *L. album* hairy root culture in a dose-dependent manner. Zhang et al. (2008) showed that the NaHS pre-treatment increases the accumulation of all free amino acids in wheat seeds exposed to copper stress. They also suggested an important function for H_2S in the mobilization of protein supply. Herein, the profiling of amino acids in response to the NaHS was separately considered because the defense networks are regulated by secondary metabolites, amino acids and carbohydrates (Trouvelot et al., 2014; Zeier, 2013).

In the present investigation, several essential amino acids are found at low levels (*e.g.*, phenylalanine, tyrosine, valine, serine, glutamate, aspartate and arginine), or at high levels (*e.g.*, histidine and proline) in hairy roots treated with 1 mM NaHS (Fig. 7). A decrease in the contents of tyrosine and phenylalanine, a substrate respectively for TAL and PAL, was consistent with an increased flux of the phenylpropanoid pathways. In this study, the NaHS treatment was shown to stimulate the histidine accumulation and to promote the proline content. The Histidine can act as scavenger for both hydroxyl radical and singlet oxygen (Wade and Tucker, 1998). Moreover, an imidazole moiety in histidine-containing peptide mediates inhibition of lipid peroxidation through a hydrogen donation for lipid radical trapping (Chi et al., 2015); therefore, the histidine spike after the NaHS treatment might contribute to the antioxidant activity. The decrease of glutamate content is related to its precursory role in the biosynthesis of proline as a key molecule in the maintenance of plasma membrane integrity and the protection of enzymes against denaturation and as a reservoir of carbon and nitrogen

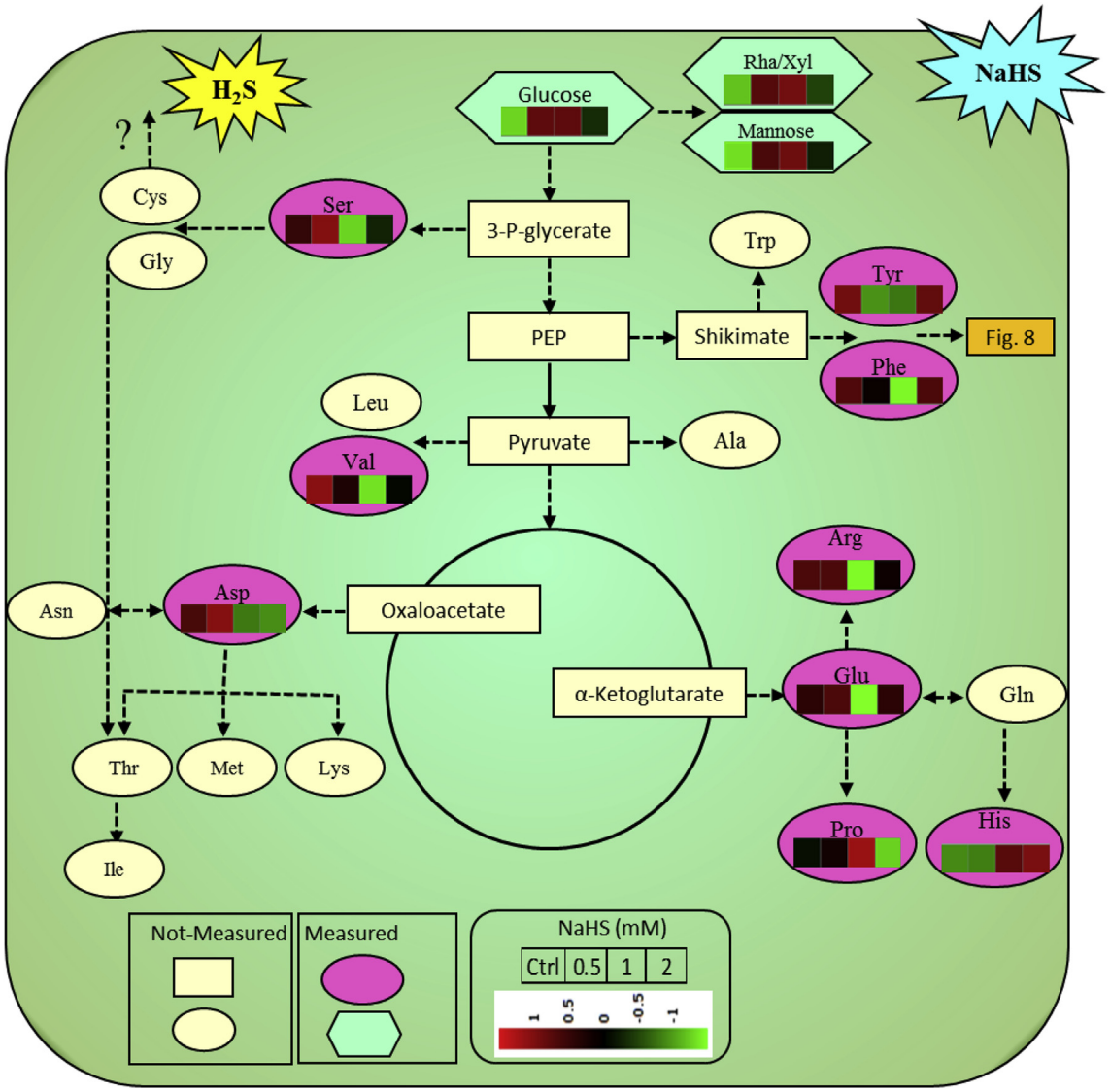

Fig. 7. Schematic representation of synthetic pathways for synthesis of amino acids in plants. Heat maps indicate log 2 -transformed values of the concentrations of metabolites in hairy roots treated with different concentration of NaHS (0.5, 1, and 2 mM). Arrows indicate the order of steps in the pathway; dashed arrows represent multiple enzymatic steps linking metabolites (squares) to amino acid (ellipses). Pink and light yellow indicate the measured and not-measured compounds by HPLC, respectively. Light blue hexagons indicate simple sugars. (For interpretation of the references to color in this figure legend, the reader is referred to the Web version of this article.)

(Bagdi and Shaw, 2013). In plants, serine is predominantly generated during the overall process of photorespiration (Bauwe et al., 2010) and is highly active as a metabolic signal in plants (Benstein et al., 2013). Serine is also a precursor for the biosynthesis of a multitude of metabolites such as amino acids glycine, cysteine, and tryptophan (Fig. 7). The genes involved in the 'phosphorylated' pathway (Cascales-Minana et al., 2013) are highly expressed in non-photosynthetic tissues like roots or in the regions of primary meristems. In bacteria and plants, cysteine is generated from serine (via acetylserine), and degraded to produce H_2S, amine and pyruvate (Li, 2013), which respond to environmental stress and induce the acquisition of stress tolerance. In addition, the cysteine amino acid is very reactive if it is allowed to accumulate above a certain level; therefore, the cysteine conversion to H_2S can serve as a detoxification mechanism, released to air (Li, 2013). Our results showed an increase in the serine accumulation of 0.5 mM NaHS and a significant decrease for both 1 and 2 mM NaHS. It was hypothesized that the serine accumulation in hairy roots after the NaHS treatment is a way to the cysteine production and to maintain H_2S as a signal molecule in a positive loop. Most amino acids were grouped in cluster 2 with similar profiles of the fold change patterns in response to NaHS-inducible oxidative stress of hairy root culture of *L. album* (Fig. 6B).

4.3. H_2S diverts the phenylpropanoid metabolism toward lignans

Plants respond to stresses through activating signaling cascades at first. Consequently, it leads to the initiation of the enzymatic (antioxidant enzymes) and non-enzymatic (such as phenolic and flavonoid compounds) antioxidant defense systems (Racchi, 2013). Stresses can also lead to the shift from primary to secondary metabolism, and the production of secondary metabolites that are silent during replicative growth (Selmar and Kleinwachter, 2013). There are some reports on the stimulatory effect of H_2S on metabolite production in plants. As an instance, the contents of phenolics and flavonoids in banana peel increased after H_2S treatment (Ge et al., 2017). Hydrogen sulfides also induced nicotine biosynthesis in tobacco (Chen et al., 2016). On the other hand, the previous findings in our lab focused on the effects of various elicitors in the cell and hairy root culture of *L. album* and on the

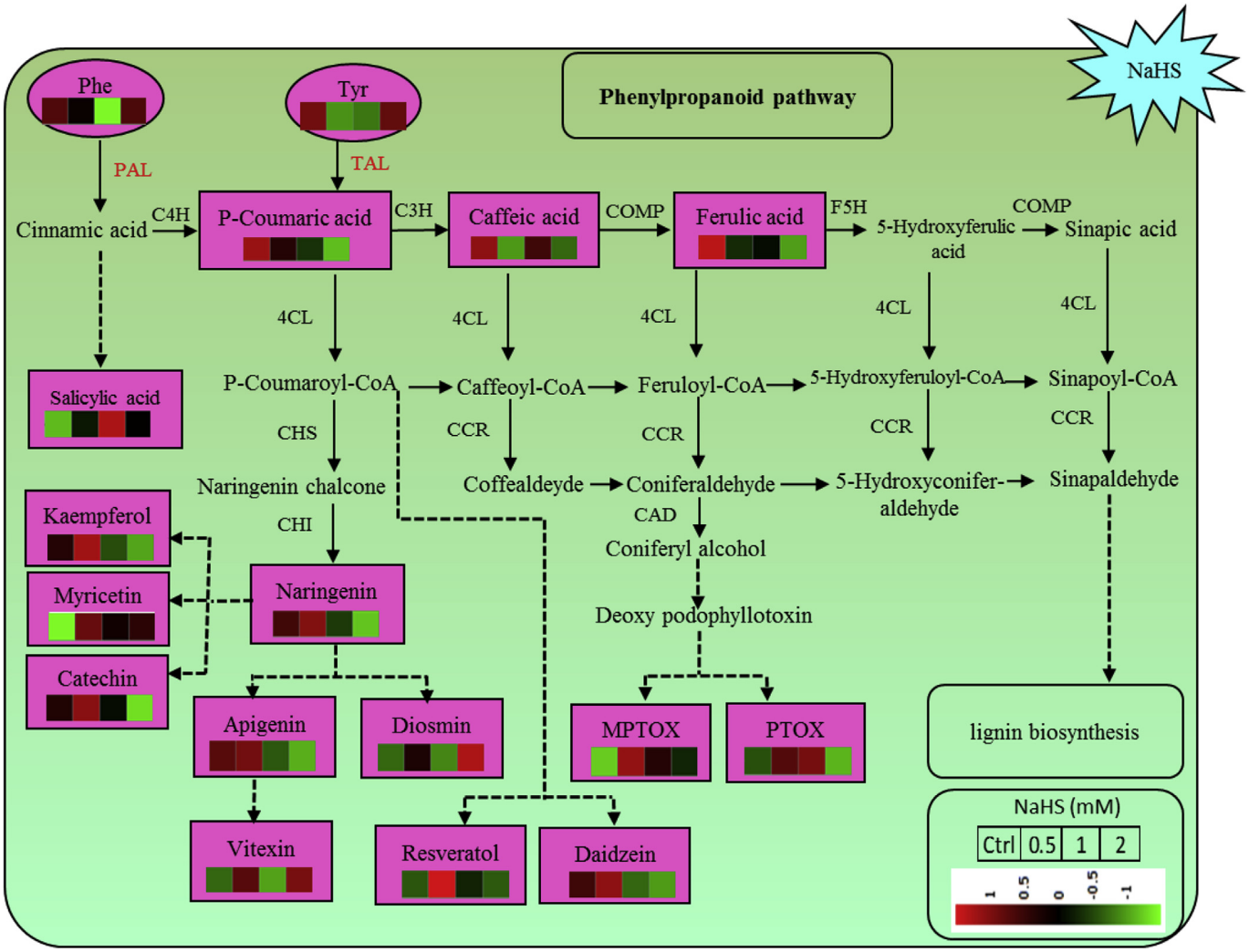

Fig. 8. Metabolic profiling of hairy roots of *L. album*. The schematic diagram shows the branches of the phenylpropanoid pathway involved in flavonoid and lignan. Heat maps indicate log 2 -transformed values of the concentrations of metabolites in hairy roots treated with different concentration of NaHS (0, 0.5, 1, and 2 mM). Arrows indicate the order of steps in the pathway; dashed arrows represent multiple enzymatic steps. Pink ellipses indicate the measured amino acids by HPLC. Pink squares indicate metabolites identified in response to NaHS. Among main enzymes of the phenylpropanoids pathway, the measured PAL and TAL activities was shown with red color. The main enzymes are as follows: C4H, cinnamate 4-hydroxylase; 4CL, 4-coumaroyl-CoA ligase; CHS, chalcone synthase; CHI, chalcone isomerase; C3H, p-coumaroyl ester 3-hydroxylase; COMT, caffeic acid O-methyltransferase; CAD, cinnamyl alcohol dehydrogenase; CCR, cinnamoyl-CoA reductase; F5H, ferulic acid 5-hydroxylase; PAL, phe ammonia lyase; TAL, tyrosine ammonia lyase. (For interpretation of the references to color in this figure legend, the reader is referred to the Web version of this article.)

content of phenylpropanoid compounds (Yousefzadi et al., 2010; Esmaeilzadeh Bahabadi et al., 2014; Tashackori et al., 2016). Herein, we present evidence that H_2S may be involved in the biosynthesis of lignans, flavonoids, carbohydrate, phenolic and amino acids. Since hairy root culture of *L. album* has high potential in the accumulation of lignans, we could observe an increase in the contents of PTOX and 6-MPTOX at non-toxic concentration of NaHS. These findings considered the use of H_2S as a new elicitor to improve production of medicinally benefit lignans compared with the previously applied biotic and abiotic elicitors. We also observed that the NaHS induced the SA accumulation (Fig. 8). Previous findings in our lab also demonstrated that the external application of the SA alone could induce the biosynthesis of PTOX in the cell culture of *L. album* (Yousefzadi et al., 2010). SA is one of the key phytohormones for resistance to abiotic and biotic stresses (Dong et al., 2014), therefore it can be hypothesized that the H_2S transiently acts as the upstream signal of the SA. Chen et al. (2016) reported that the exogenous H_2S donor, NaHS, increased nicotine biosynthesis in tobacco through crosstalk with JA, where the H_2S may act upstream of the JA signaling. The JA also has a stimulatory role in the production of PTOX in the cell culture of *L. album* (Esmaeilzadeh Bahabadi et al., 2014).

The biosynthesis of lignans and flavonoids are controlled by PAL activity. It converts the phenylalanine to trans-cinnamic acid and causes the shift from primary to secondary metabolism (Sreelakshmi and Sharma, 2008). The increase of PTOX accumulation can be correlated to the decrease of central intermediates in the phenylpropanoid pathway, including coumaric, caffeic, and ferulic acids, which are substrates for PTOX and 6-MPTOX biosynthesis (Fig. 8). Moreover, the changes in the flavonoids upon NaHS treatment were dose-dependent (Fig. 8). In plants, there have been few reports on the relationship between flavonoids and H_2S. Recently, Li et al. (2016) found that the H_2S production in the leaves of barley seedlings was induced by UV-B radiation and accumulated flavonoids and anthocyanins. In our study, most of identified flavonoids decreased after 5 d of exposure; but the lignans accumulated in hairy root culture of *L. album* when NaHS was applied. Accordingly, it was hypothesized that the H_2S leads to the shift from flavonoid to lignan pathway. The shift may be caused by alterations in gene transcription, enzyme expression, and gene regulation (an issue of further investigation). An enhancement of the flavonoid

contents (Fig. S2) and 6-MPTOX can be seen under 0.5 mM NaHS treatment. The hairy root culture of *L. album* accumulated the PTOX, 6MPTOX, or both of them as main lignans. Deoxypodophyllotoxin is the precursor and branching point to PTOX or 6-MPTOX generation. If hydroxylation of deoxypodophyllotoxin occurs at position 7 by deoxypodophyllotoxin 7-hydroxylase (DOP7H), the PTOX is the reaction product. On the other hand, hydroxylation at position 6 of deoxypodophyllotoxin leads to the biosynthesis of 6-MPTOX (via beta-peltatin), by the deoxypodophyllotoxin 6-hydroxylase a cytochrome p450 dependent monooxygenase (Molog et al., 2001). It is therefore possible that cytochrome P450 regulates the biosynthesis of 6-MPTOX in the presence of H_2S.

5. Conclusion

Hydrogen sulfide (H_2S) is a signaling molecule in the root architecture development. The H_2S application to the hairy root culture of *L. album* changed the metabolic profiles and caused a shift from primary to secondary metabolism, possibly due to the production of bioactive compounds, such as H_2O_2, NO, and SA. In addition, the H_2S modulate osmolytes and antioxidant system in hairy root culture of *L. album*. The central intermediates in the phenylpropanoid pathway, such as phenolic acids, decreased in response to NaHS and the lignan biosynthesis is favored over flavonoids. These results showed that H_2S and the studied signaling molecules could play a synergistic role in the production of lignans such as PTOX and 6-PTOX. Therefore, the application of H_2S alone or together with the other signaling molecules could be commercially useful to enhance phenylpropanoids biosynthesis.

Conflicts of interest

The authors have no conflict of interest to report.

CRediT authorship contribution statement

Safieh Fakhari: Formal analysis, Writing – original draft. **Mohsen Sharifi:** Supervision, Writing – review & editing. **Roberto De Michele:** Writing – review & editing. **Faezeh Ghanati:** Writing – review & editing. **Naser Safaie:** Methodology. **Ehsan Sadeghnezhad:** Formal analysis, Writing – original draft, Writing – review & editing.

Acknowledgments

The research is financed by grant from Tarbiat Modares University, Tehran, Iran.

Appendix A. Supplementary data

Supplementary data to this article can be found online at https://doi.org/10.1016/j.plaphy.2018.12.015.

References

Ahmadian Chashmi, N., Sharifi, M., Yousefzadi, M., Behmanesh, M., Rezadoost, H., Cardillo, A., Palazon, J., 2013. Analysis of 6-methoxy podophyllotoxin and podophyllotoxin in hairy root cultures of *Linum album* Kotschy ex Boiss. Med. Chem. Res. 22, 745–752.

Akkol, E.K., Göger, F., Kosar, M., Baser, K.H., 2008. Phenolic composition and biological activities of *Salvia halophile* and *Salvia virgata* from Turkey. Food Chem. 108 (3), 942–949.

Apel, K., Hirt, H., 2004. Reactive oxygen species: metabolism, oxidative stress, and signal transduction. Annu. Rev. Plant Biol. 55, 373–399.

Ayres, D.C., Loike, J.D., 1990. Lignans Chemical, Biological and Clinical Properties. Cambridge University Press, Cambridge.

Baek, D., Pathange, P., Chung, J.S., Jiang, J., Gao, L., Oikawa, A., Hirai, M.Y., Saito, K., Pare, P.W., Shi, H., 2010. A stress – inducible sulphotransferase sulphonates salicylic acid and confers pathogen resistance in Arabidopsis. Plant Cell Environ. 33, 1383–1392.

Bagdi, D.L., Shaw, B.P., 2013. Analysis of proline metabolic enzymes in *Oryza sativa* under NaCl stress. J. Environ. Biol. 34 (4), 677–681.

Bates, L.S., Waldren, R.P., Teare, I.D., 1973. Rapid determination of free proline for water-stress studies. Plant Soil 39, 205–207.

Bauwe, H., Hagemann, M., Fernie, A.R., 2010. Photorespiration: players, partners and origin. Trends Plant Sci. 15 (6), 330–336.

Benstein, R.M., Ludewig, K., Wulfert, S., Wittek, S., Gigolashvili, T., Frerigmann, H., Gierth, M., Flügge, U.I., Krueger, S., 2013. Arabidopsis phosphoglycerate dehydrogenase1 of the phosphose-serine pathway is essential for development and required for ammonium assimilation and tryptophan biosynthesis. Plant Cell 25 (12), 5011–5029.

Biermann, M., Bardl, B., Vollstadt, S., Linnemann, J., Knüpfer, U., Seidel, G., Horn, U., 2013. Simultaneous analysis of the non-canonical amino acids norleucine and norvaline in biopharmaceutical-related fermentation processes by a new ultra-high performance liquid chromatography approach. Amino Acids 44 (4), 1225–1231.

Bolton, M.D., 2009. Primary metabolism and plant defense–fuel for the fire. Mol. Plant Microbe Interact. 22, 487–497.

Bradford, M.M., 1976. A rapid and sensitive method for the quantitation of microgram quantities of protein utilizing the principle of protein-dye binding. Anal. Biochem. 72, 248–254.

Cakmak, I., Marschner, H., 1992. Magnesium deficiency and high light intensity enhance activities of superoxide dismutase, ascorbate peroxidase, and glutathione reductase in bean leaves. Plant Physiol. 98 (4), 1222–1227.

Cascales-Minana, B., Munoz-Bertomeu, J., Flores-Tornero, M., Anoman, A.D., Pertusa, J., Alaiz, M., Osorio, S., Fernie, A.R., Segura, J., Ros, R., 2013. The phosphorylated pathway of serine biosynthesis is essential both for male gametophyte and embryo development and for root growth in Arabidopsis. Plant Cell 25 (6), 2084–2101.

Chance, B., Maehly, A.C., 1955. Assay of catalase and peroxidase. Methods Enzymol. 2, 764–775.

Chen, J., Wang, W.H., Wu, F.H., He, E.M., Liu, X., Shangguan, Z.P., Zheng, H.L., 2015. Hydrogen sulfide enhances salt tolerance through nitric oxide-mediated maintenance of ion homeostasis in barley seedling roots. Sci. Rep. 5, 12516.

Chen, X., Chen, Q., Zhang, X., Li, R., Jia, Y., Ef, A., Jia, A., Hu, L., Hu, X., 2016. Hydrogen sulfide mediates nicotine biosynthesis in tobacco (*Nicotiana tabacum*) under high temperature conditions. Plant Physiol. Biochem. 104, 174–179.

Chi, C.F., Hu, F.Y., Wang, B., Li, Z.R., Luo, H.Y., 2015. Influence of amino acid compositions and peptide profiles on antioxidant capacities of two protein hydrolysates from Skipjack Tuna (*Katsuwonus pelamis)* dark muscle. Mar. Drugs 13, 2580–2601.

Clark, N.R., Ma'ayan, A., 2011. Introduction to statistical methods to analyze large data sets: principal components analysis. Sci. Signal. 4 (190), tr3 6.

Das, K., Roychoudhury, A., 2014. Reactive oxygen species (ROS) and response of antioxidants as ROS-scavengers during environmental stress in plants. Front Environ. Sci. 2, 53.

De Michele, R., Vurro, E., Rigo, C., Costa, A., Elviri, L., Di Valentin, M., Careri, M., Zottini, M., di Toppi, L.S., Schiavo, F., 2009. Nitric Oxide is involved in cadmium-induced programmed cell death in Arabidopsis suspension cultures. Plant Physiol. 150, 217–228.

Di Martino, C., Delfine, S., Pizzuto, R., Loreto, F., Fuggi, A., 2003. Free amino acids and glycine betaine in leaf osmoregulation of spinach responding to increasing salt stress. New Phytol. 158, 455–463.

Dong, C.J., Li, L., Shang, Q.M., Liu, X.Y., Zhang, Z.G., 2014. Endogenous salicylic acid accumulation is required for chilling tolerance in cucumber (*Cucumis sativus* L.) seedlings. Planta 240, 687–700.

Dorman, D.C., Moulin, F.J., McManus, B.E., Mahle, K.C., James, R.A., Struve, M.F., 2002. Cytochrome oxidase inhibition induced by acute hydrogen sulfide inhalation: correlation with tissue sulfide concentrations in the rat brain, liver, lung, and nasal epithelium. Toxicol. Sci. 65 (1), 18–25.

Du, X., Zhang, C., Guo, W., Jin, W., Liang, Z., Yan, X., Guo, Z., Liu, Y., Yang, D., 2015. Nitric oxide plays a central role in water stress-induced tanshinone production in *Salvia miltiorrhiza* hairy roots. Molecules 20, 7574–7585.

DuBois, M., Gilles, K.A., Hamilton, J.K., Rebers, P.A., Smith, F., 1956. Colorimetric method for determination of sugars and related substances. Anal. Chem. 28, 350–356.

Edwards, P.M., 2002. Origin 7.0: scientific graphing and data analysis software. J. Chem. Inf. Comput. Sci. 42 (5), 1270–1271.

Esmaeilzadeh Bahabadi, S., Sharifi, M., Ahmadian Chashmi, N., Murata, J., Satake, H., 2014. Significant enhancement of lignan accumulation in hairy root cultures of *Linum album* using biotic elicitors. Acta Physiol. Plant. 36, 3325–3331.

Falcone Ferreyra, M.L., Rius, S.P., Casati, P., 2012. Flavonoids: biosynthesis, biological functions, and biotechnological applications. Front. Plant Sci. 28 (3), 222.

Federolf, K., Alfermann, A.W., Fuss, E., 2007. Aryltetralin-lignan formation in two different cell suspension cultures of *Linum album*: deoxypodophyllotoxin 6-hydroxylase, a key enzyme for the formation of 6-methoxy podophyllotoxin. Phytochemistry 68, 1397–1406.

Ge, Y., Hu, K.D., Wang, S.S., Hu, L.Y., Chen, X.Y., Li, Y.H., Yang, Y., Yang, F., Zhang, H., 2017. Hydrogen sulfide alleviates postharvest ripening and senescence of banana by antagonizing the effect of ethylene. PLoS One 12 (6), e0180113.

Giannopolitis, C.N., Ries, S.K., 1977. Superoxide dismutases: I. occurrence in higher plants. Plant Physiol. 59, 309–314.

Gordaliza, M., Garcia, P.A., Del Corral, J.M., Castro, M.A., Gomez-Zurita, M.A., 2004. Podophyllotoxin: distribution, sources, applications and new cytotoxic derivatives. Toxicon 44, 441–459.

Green, L.C., Wagner, D.A., Glogowski, J., Skipper, P.L., Wishnok, J.S., Tannenbaum, S.R., 1982. Analysis of nitrate nitrite and [15 N] nitrate in biological fluids. Anal. Biochem. 126 (1), 131–138.

Gudej, J., Tomczyk, M., 2004. Determination of flavonoids, tannins and ellagic acid in

leaves from Rubus L. species. Arch Pharm. Res. 27, 1114–1119.
Hancock, J.T., Whiteman, M., 2014. Hydrogen sulfide and cell signaling: team player or referee? Plant Physiol. Biochem. 78, 37–42.
Hasanuzzaman, M., Bhuyan, M.H.M.B., Mahmud, J.A., Nahar, K., Mohsin, S.M., Parvin, K., Fujita, M., 2018. Interaction of sulfur with phytohormones and signaling molecules in conferring abiotic stress tolerance to plants. Plant Signal. Behav. 13 (5), e1477905.
Hu, H., Shen, W., Li, P., 2014. Effects of hydrogen sulphide on quality and antioxidant capacity of mulberry fruit. Int. J. Food Sci. Technol. 49, 399–409.
Jia, H., Hu, Y., Fan, T., Li, J., 2015. Hydrogen sulfide modulates actin-dependent auxin transport via regulating ABPs results in changing of root development in Arabidopsis. Sci. Rep. 5, 8251.
Kadotani, N., Akagi, A., Takatsuji, H., Miwa, T., Igarashi, D., 2016. Exogenous proteinogenic amino acids induce systemic resistance in rice. BMC Plant Biol. 16, 60.
Keinanen, M., Oldham, N.J., Baldwin, I.T., 2001. Rapid HPLC screening of jasmonate -induced increases in tobacco alkaloids, phenolics, and diterpene glycosides in *Nicotiana attenuata*. J. Agric. Food Chem. 49, 3553–3558.
Lee, Y.P., Takahashi, T., 1966. An improved colorimetric determination of amino acids with the use of ninhydrin. Anal. Biochem. 14, 71–77.
Li, Z.G., 2013. Hydrogen sulfide: a multifunctional gaseous molecule in plants. Russ. J. Plant Physiol. 60, 733–740.
Li, Z.G., Ding, X.J., Du, P.F., 2013. Hydrogen sulfide donor sodium hydrosulfide improved heat tolerance in maize and involvement of proline. J. Plant Physiol. 170 (8), 741–747.
Li, Z.G., Xie, L.R., Li, X.J., 2015. Hydrogen sulfide acts as a downstream signal molecule in salicylic acid-induced heat tolerance in maize (*Zea mays* L.) seedlings. J. Plant Physiol. 177, 121–127.
Li, Q., Wang, Z., Zhao, Y., Zhang, X., Zhang, S., Bo, L., Wang, Y., Ding, Y., An, L., 2016. Putrescine protects hulless barley from damage due to UV-B stress via H_2S- and H_2O_2-mediated signaling pathways. Plant Cell Rep. 35 (5), 1155–1168.
Lindermayr, C., Sell, S., Muller, B., Leister, D., Durner, J., 2010. Redox regulation of the NPR1-TGA1 system of *Arabidopsis thaliana* by nitric oxide. Plant Cell 22, 2894–2907.
Mei, Y., Chen, H., Shen, W., Shen, W., Huang, L., 2017. Hydrogen peroxide is involved in hydrogen sulfide-induced lateral root formation in tomato seedlings. BMC Plant Biol. 17 (1), 162.
Molog, G.A., Empt, U., Kuhlmann, S., Van Uden, W., Pras, N., Alfermann, A.W., Petersen, M., 2001. Deoxypodophyllotoxin 6-hydroxylase, a cytochrome P450 monooxygenase from cell cultures of *Linum flavum* involved in the biosynthesis of cytotoxic lignans. Planta 214, 288–294.
Montesinos-Pereira, D., Barrameda-Medina, Y., Baenas, N., Moreno, D.A., Sánchez-Rodríguez, E., Blasco, B., Ruiz, J., 2016. Evaluation of hydrogen sulfide supply to biostimulate the nutritive and phytochemical quality and the antioxidant capacity of Cabbage (*Brassica oleracea* L. 'Bronco'). J. Appl. Bot. Food Qual. 89, 290–298.
Murashige, T., Skoog, F., 1962. A revised medium for rapid growth and bio assays with tobacco tissue cultures. Physiol. Plantarum 15, 473–497.
Nahidian, B., Ghanati, F., Shahbazi, M., Soltani, N., 2018. Effect of nutrients on the growth and physiological features of newly isolated *Haematococcus pluvialis* TMU1. Bioresour. Technol. 255, 229–237.
Namdeo, A.G., 2007. Pharmacognosy reviews plant cell elicitation for production of secondary metabolites: a review. Phcog. Rev. 1, 69–79.
Nazar, R., Umar, S., Khan, N.A., 2015. Exogenous salicylic acid improves photosynthesis and growth through increase in ascorbate-glutathione metabolism and S assimilation in mustard under salt stress. Plant Signal. Behav. 10, e1003751.
Owen, R.W., Haubner, R., Mier, W., Giacosa, A., Hull, W.E., Spiegelhalder, B., Bartsch, H., 2003. Isolation, structure elucidation and antioxidant potential of the major phenolic and flavonoid compounds in brined olive drupes. Food Chem. Toxicol. 41, 703–717.
Pál, M., Kovács, V., Szalai, G., Soós, V., Ma, X., Liu, H., Mei, H., Janda, T., 2014. Salicylic acid and abiotic stress responses in rice. J. Agron. Crop Sci. 200, 1–11.
Peterson, J., Dwyer, J., Adlercreutz, H., Scalbert, A., Jacques, P., McCullough, M.L., 2010. Dietary lignans: physiology and potential for cardiovascular disease risk reduction. Nutr. Rev. 68 (10), 571–603.
Pareek, A., Gaur, A., Kumar, A., Lodha, P., 2017. Impacts of root knot nematode infestation on metabolites and antioxidant enzymes in *Abelmoschus esculentus* L. Moench. J. Pharmacogn. Phytochem. 6 (4), 1093–1096.
Racchi, M.L., 2013. Antioxidant defenses in plants with attention to *Prunus* and *Citrus* spp. Antioxidants 2 (4), 340–369.
Selmar, D., Kleinwachter, M., 2013. Stress enhances the synthesis of secondary plant products: the impact of stress-related over-reduction on the accumulation of natural products. Plant Cell Physiol. 54 (6), 817–826.
Shi, H., Ye, T., Chan, Z., 2014. Nitric oxide-activated hydrogen sulfide is essential for cadmium stress response in bermudagrass (*Cynodon dactylon* (L). Pers.). Plant Physiol. Biochem. 74, 99–107.
Shi, H., Ye, T., Han, N., Bian, H., Liu, X., Chan, Z., 2015. Hydrogen sulfide regulates abiotic stress tolerance and biotic stress resistance in Arabidopsis. J. Integr. Plant Biol. 57 (7), 628–640.
Shimoi, K., Masuda, S., Shen, B., Furugori, M., Kinze, N., 1996. Radio-protective effects of antioxidative plant flavonoids in mice. Mutat. Res. Fund. Mol. 350, 153–161.
Soobrattee, M.A., Neergheen, V.S., Luximon-Ramma, A., Aruoma, O.I., Bahorun, O.T., 2005. Phenolics as potential antioxidant thera-peutic agents: mechanism and actions. Mutat. Res. Fund. Mol 579, 200–213.
Sreelakshmi, Y., Sharma, R., 2008. Differential regulation of phenylalanine ammonia lyase activity and protein level by light in tomato seedlings. Plant Physiol. Biochem. 46, 444–451.
Tada, Y., Spoel, S.H., Pajerowska-Mukhtar, K., Mou, Z., Song, J., Wang, C., Zuo, J., Dong, X., 2008. Plant immunity requires conformational charges of NPR1 via S-nitrosylation and thioredoxins. Science 321, 952–956.
Tashackori, H., Sharifi, M., Ahmadian Chashmi, N., Safaie, N., Behmanesh, M., 2016. Induced-differential changes on lignan and phenolic acid compounds in *Linum album* hairy roots by fungal extract of Piriformospora indica. Plant Cell Tissue Organ Cult. 127, 187–194.
Trouvelot, S., Héloir, M.C., Poinssot, B., Gauthier, A., Paris, F., Christelle, G., Combier, M., Trdá, L., Daire, X., Adrian, M., 2014. Carbohydrates in plant immunity and plant protection: roles and potential application as foliar sprays. Front. Plant Sci. 5, 592.
Van Uden, W., Pras, N., Visser, J.F., Malingré, T.M., 1989. Detection and identification of Podophyllotoxin produced by cell cultures derived from *Podophyllum hexandrum* royle. Plant Cell Rep. 8 (3), 165–168.
Wade, A.M., Tucker, H.N., 1998. Antioxidant characteristics of L-histidine. J. Nutr. Biochem. 9 (6), 308–315.
Wang, J.W., Zheng, L.P., Wu, J.Y., Tan, R.X., 2006. Involvement of nitric oxide in oxidative burst, phenylalanine ammonia-lyase activation and Taxol production induced by low-energy ultrasound in *Taxus yunnanensis* cell suspension cultures. Nitric Oxide 15 (4), 351–358.
Wang, B.L., Shi, L., Li, Y.X., Zhang, W.H., 2010. Boron toxicity is alleviated by hydrogen sulfide in cucumber (*Cucumis sativus* L.) seedlings. Planta 231 (6), 1301–1309.
Wang, Y., Li, L., Cui, W., Xu, S., Shen, W., Wang, R., 2012. Hydrogen sulfide enhances alfalfa (*Medicago sativa*) tolerance against salinity during seed germination by nitric oxide pathway. Plant Soil 351 (1–2), 107–119.
Xie, Y., Zhang, C., Lai, D., Sun, Y., Samma, M.K., Zhang, J., Shen, W., 2014. Hydrogen sulfide delays GA-triggered programmed cell death in wheat aleurone layers by the modulation of glutathione homeostasis and heme oxygenase-1expression. J. Plant Physiol. 171 (2), 53–62.
Yamasaki, H., Cohen, M.F., 2016. Biological consilience of hydrogen sulfide and nitric oxide in plants: gases of primordial earth linking plant, microbial and animal physiologies. Nitric Oxide 55, 91–100.
Yousefzadi, M., Sharifi, M., Behmanesh, M., Ghasempour, A., Moyano, E., Palazon, J., 2010. Salicylic acid improves podophyllotoxin production in cell cultures of *Linum album* by increasing the expression of genes related with its biosynthesis. Biotechnol. Lett. 32 (11), 1739–1743.
Zafari, S., Sharifi, M., Chashmi, N.A., Mur, L.A., 2016. Modulation of Pb-induced stress in Prosopis shoots through an interconnected network of signaling molecules, phenolic compounds and amino acids. Plant Physiol. Biochem. 99, 11–20.
Zafari, S., Sharifi, M., Mur, L.A., Ahmadian Chashmi, N., 2017. Favouring NO over H_2O_2 production will increase Pb tolerance in *Prosopis farcta* via altered primary metabolism. Ecotoxicol. Environ. Saf. 142, 293–302.
Zeier, J., 2013. New insights into the regulation of plant immunity by amino acid metabolic pathways. Plant Cell Environ. 36, 2085–2103.
Zg, L., Xj, D., Pf, D., 2013. Hydrogen sulfide donor sodium hydrosulfide-improved heat tolerance in maize and involvement of proline. J. Plant Physiol. 170, 741–747.
Zhang, H., Hu, L.Y., Hu, K.D., He, Y.D., Wang, S.H., Luo, J.P., 2008. Hydrogen sulfide promotes wheat seed germination and alleviates oxidative damage against copper stress. J. Integr. Plant Biol. 50 (12), 1518–1529.
Zhang, H., Tang, J., Liu, X.P., Wang, Y., Yu, W., Peng, W.Y., Fang, F., Ma, D.F., Wei, Z.J., Hu, L.Y., 2009. Hydrogen sulfide promotes root organogenesis in *Ipomoea batatas, Salix matsudana* and *Glycine max*. J. Integr. Plant Biol. 51 (12), 1086–1094.
Zhang, J.J., Li, X.Q., Sun, J.W., Jin, S.H., 2014. Nitric oxide functions as a signal in ultraviolet-B-induced baicalin accumulation in *Scutellaria baicalensis* suspension cultures. Int. J. Mol. Sci. 15 (3), 4733–4746.
Zhang, P., Luo, Q., Wang, R., Xu, J., 2017. Hydrogen sulfide toxicity inhibits primary root growth through the ROS-NO pathway. Sci. Rep. 7 (1), 868.
Zheng, W., Wang, S.Y., 2001. Antioxidant activity and phenolic compounds in selected herbs. J. Agric. Food Chem. 49, 5165–5170.
Zheng, L.P., Guo, Y.T., Wang, J.W., Tan, R.X., 2008. Nitric oxide potentiates oligosaccharide- induced artemisinin production in *Artemisia annua* hairy roots. J. Integr. Plant Biol. 50 (1), 49–55.
Zottini, M., Costa, A., De Michele, R., Ruzzene, M., Carimi, F., Lo Schiavo, F., 2007. Salicylic acid activates nitric oxide synthesis in Arabidopsis. J. Exp. Bot. 58 (6), 1397–1405.